2011 International Conference on Transportation, Mechanical, and Electrical Engineering (TMEE)
December 16-18, Changchun, China

Pavement distress detection and classification with automated image processing

Xiaoming Wang
School of Electrical and Information Engineering,
Lanzhou University of Technology
Lanzhou,Gansu,China,730050
majing111111@sina.com

Xin Feng
School of Electrical and Information Engineering,
Lanzhou University of Technology
Lanzhou,Gansu,China,730050
149495263@qq.com

***Abstract*—nowadays, pavement distresses classification becomes more important as the computational power increases. In this article, an enhancement algorithm is initially introduced to remove uneven illumination within the pavement images. This proposed method which uses a multiplicative factor to correct the background illumination, after that use shearlet frame to filtering the pavement images. In the classification of operation, we used Radon transform for line and angle detection about pavement distress of binary images, and use scattering distance to verify the result of classification by the texture feature of pavement distress images. Experimental results demonstrate that the proposed system is an effective method for pavement distress classification. The test performances of this study show the advantages of proposed system:have simple calculation, and have High precision.**

Keywords-pavement distresses classification; shearlet; Radon transform; scattering distance

I. INTRODUCTION

Pavement detection is a key and basic technology in the highway construction and management. It is very necessary for us to develop a automatic detection system of pavement distress which is fast, objective and relatively cheap for the present transportation network system[1].

Machine vision and image processing technology as a tool to have been integrated into the many of the field and have the most significant achievements in the medical and remote sensing at present[2]. The application of this technology in transportation is also developed very fast,many countries have applied the image analysis and pattern recognition to detect the pavement distresses at present[3]. The main pavement detection system is use the camera which is installed on the mobile of vehicle to get the image, and then through the computer to automatic recognition and quantification the images.

Cheng,Glazier, and Hu (1999)[4]used Hough Transform (HT) to determine the type of the crack. Hsu, Chen, Lee and Huang (2001)[5], described a moment invariant technique for feature extraction and a NN for crack classification. The moment invariant technique reduces a two dimensional image pattern into feature vectors that characterize the image such as:translation,scale, rotation of an object in an image. After these features are extracted the overall results of this study were satisfactory and the classification accuracy of the introduced system was 85%. Zhou, Huang and Chiang (2006)[6]proposes several statistical criteria are developed for distress detection and isolation, which include the High Amplitude Wavelet Coefficient Percentage (HAWCP), the High Frequency Energy Percentage (HFEP), and the standard deviation (STD). These criteria are tested on hundreds of pavement images differing by type, severity, and extent of distress.Experimental results demonstrate that the proposed criteria are reliable for distress detection and isolation and that real-time distress detection and screening is feasible. Sorncharean and Phiphobmongkol (2008)[7]is proposed a novel pavement image thresholding algorithm based on neighboring difference histogram method (NDHM). Sorncharean and Phiphobmongkol (2008)[7]presents image processing techniques based on grid cell analysis for crack detection on non-uniform illumination and strong texture images. Wang (2008)[8] using wavelet edge detection based on a Trous algorithm (holes algorithm) is used in pavement distress segmentation. This algorithm is an undetermined wavelet transform executed via a filter bank without sub-sampling process. By comparisons with the results derived from five other traditional edge detectors, the study demonstrates the validity and effectiveness of this method for edge detection of pavement surface distresses. Pavement. Distress classification method improved in this paper consist of five stages: (1) image enhancement, (2) shearlet de-noising, (3) Radon Transform for classification, (4) scattering transform for Texture feature matching. The system structure of this paper is as follows:

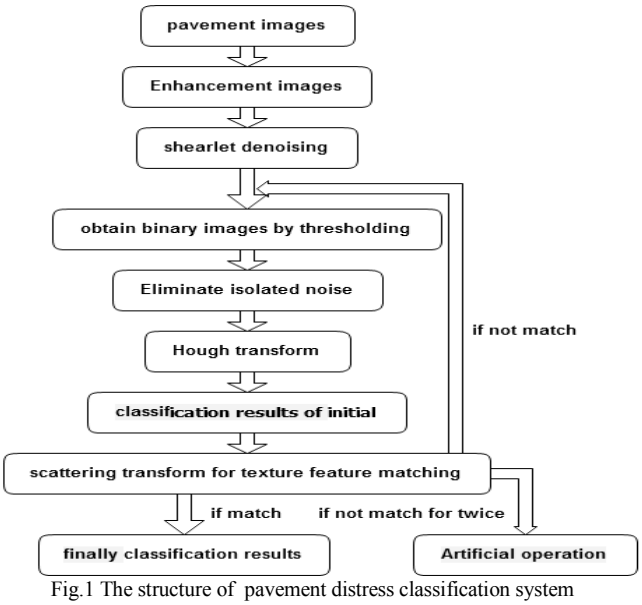

Fig.1 The structure of pavement distress classification system

II. IMAGE ENHANCEMENT

The strength of matrix about the image of the crack of pavement contains three changes:

- High-amplitude, low-frequency non-uniform background component ;
- High-amplitude, and high-frequency pavement distress or non-distress irregularities component;
- A random, low-to-medium amplitude, high-frequency noise component, caused by heterogeneous materials and granularity;

In 1998, Cheng, H. D. and Miyojim, M.[9]proposed a multiply factor method. First of all, pavement image are divided into rectangle windows, the mean value of each window is checked, and then a multiplier is computed for each window which can transfer the mean value of each window to a target value. This method is based on the assumption that the illumination of the pavement image is smoothly changed. When there is a sudden drop, the window is considered to have cracks, and the mean value of this window is replaced by the average of neighboring windows. However, if there are cracks that cross more than one window, this algorithm doesn't work. In this thesis, based on Cheng, H. D. and Miyojim, M.'s work, a new non-uniform background removal method is proposed below.

1) Partition the image into rectangular windows. The size of the window can vary with the size and type of the input images.

2) For each window, calculate the mean G_{mean} minimum $G_{\min}$ and the maximum $G_{\max}$ gray level.

3) For each window, set an upper limit (r_h) and a lower limit (r_l) for which the points with gray levels outside the limits are considered as suspicious points for noise, crack pixels, or other objects on the road.The range [r_h , r_l] is determined by the following equations:

$$r_h = G_{mean} + (G_{\max} - G_{mean}) \times f \quad (1)$$

$$r_l = G_{mean} + (G_{mean} - G_{\min}) \times f \quad (2)$$

where f is the limiting factor. It can be varied for different images. From experiments, we set the limiting factor to be 0.6.

4) With the exemption of the suspicious points, recalculate the mean value of the gray level G'_{mean} .Note that G'_{mean} is the updated mean value of each window,without the factors of noises and crack pixels.

5) The amplitude correction factor is calculated as, $F = B / G_{mean}$, where B is the target background value, and in experiments, the mean value of the original image is used as B. Then the modified picture is obtained by multiplying the factor to each point of the original picture $I' = I \times f$,where, I' is the improved image. The image after enhancement gives a uniform background in both x and y directions. However, if there are many crack pixels in a window, the intensity of the non-crack pixels may increase. Thus, for the pixels whose intensity values are higher than B, their original values either remain unchanged or are replaced by the value B.

Figure 2 (a) and (c) respectively show the the non-uniform images of pavement background.Figure 1 (b) and (d) shows the pavement images of after background uniformity .We use the gray image of the size is 512 * 512 for original image, and the rectangular window size is 4*4.Obviously, The small stones and road surface crack strength of the block be processed very uniform,make for removing noise the next stage.

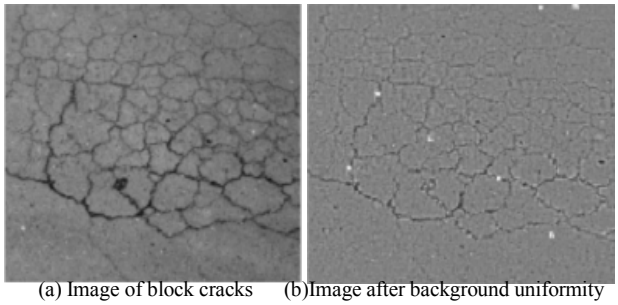

(a) Image of block cracks (b)Image after background uniformity

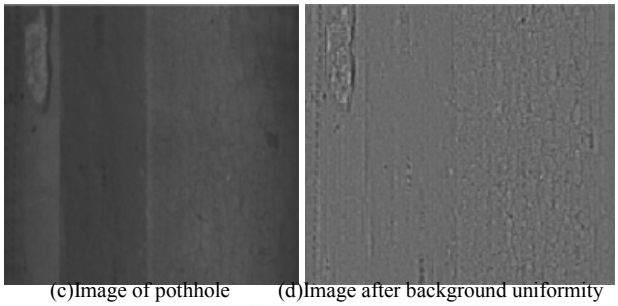

(c)Image of pothhole (d)Image after background uniformity

Fig.2 Background uniformity of pavement crack image

III. SHEARLET DE-NOISING

One of the most common shortcomings of the frameworks of the system curverlet and contourlet is lack of providing a unified treatment of the continuum and digital world[10]. To meet the unity is must have the following properties:(1) Parseval Frame Property; (2) Isometry of Pseudo-Polar Fourier Transform; (3) Space-Frequency-Localization;(4) True Shear Invariance;(5) speed; (6) Geometric Exactness; (7) Robustness; Shearlet systems are the only systems so far which satisfy this property, yet still deliver optimally sparse approximations of images.So we use it for the image denoising.

A. The frame of Shearlet

The frame of shearlet is:

$$\psi^0 = \left\{ \psi^i_{ikj} : j,k \in \mathbb{Z}, m \in \mathbb{Z}^2, i = 1,\ldots,L \right\} \quad (3)$$

$$\psi = \left\{ T_{cm}\phi : m \in \mathbb{Z}^2 \right\} \cup \left\{ \psi^i_{ikj} : j \geq 0, -s_j \leq k \leq s_j, m \in \mathbb{Z}^2, i = 1,\ldots,L \right\} \cup \left\{ \tilde{\psi}^i_{ikj} : j \geq 0, -s_j \leq k \leq s_j, m \in \mathbb{Z}^2, i = 1,\ldots,L \right\} \quad (4)$$

Where $\psi^i_{ikj} = D_{A_0^{-j} B_0^{-k}} T_{cm} \varphi^i_0$,

$\tilde{\psi}^i_{ikj} = D_{A_1^{-j} B_1^{-k}} T_{cm} \varphi^i_1$, when ψ

(or ψ^0) is the frame of the shearlet, and the functions ψ^{i}_{ikj} and $\tilde{\psi}^{i}_{ikj}$ are the shearlet of the system ψ(or ψ^0).

B. (FDST)Fast digital shearlet transform

Fast digital shearlet transform is consists of fast PPFT (fast pseudo-polar Fourier transform) ,Weighting, and Digital Shearlet Windowing.The reconstruction of the transformation can be composed by two process, respectively adjoint FDST transformation and IFDFT transform. There are two possibilities: the Adjoint FDST and the Inverse FDST depending on whether the weighting allows to use the adjoint for reconstruction or whether an iterative procedure is required for higher accuracy.

C. SURE-FDST denoising

The frame of shearlet can sparse representation for the geometric structure of images, and keep more important information of the edges and texture of the images.But need to determine the threshold before remove the noise in the process of the denoising. So the threshold choice still has a big effect to the results of denoising. Instead, SURE-LET not need to determine the threshold of denoising beforehand, but it not consider the expression of the geometric structure of the images.Therefore, this paper combine shearlet framework and SURE-LET noise estimates that can not only in the frequency domain to the satisfaction of localized, but also can not dependent on noise image. It can achieve better effect by minimize the MSE of images and the standard images.

Step1:First of all, decompose the images by SURE-LET, set $K = 2$, $T = \sqrt{6}\sigma$, σ is the noise variance, and decomposition level of the image is $J = \log_2 N - 1$. After that, obtain the predicted value y_p by GDC(group delay compensated) and Gaussian smooth. Finally get the functions $\theta(.)$ which can make the MSE minium.

Step2:Do fast PPFT to the images.

Step3:Calculation the square root of the function w after transformation.

Step4:Apply the shearlet windows to the function wPI , followed by a 2D iFFT to each array to obtain the shearlet coefficients $c^{l}_{j,k,m}$, $c^{l_0}_{n_0}$.

Step5:According to the results of the first step calculate the function $\theta(y_i, y_{ip})$ which can minimize MSE. Deal with shearlet coefficients $c^{l}_{j,k,m}$, $c^{l_0}_{n_0}$, and get the optimal shearlet coefficient.

Step6:According to whether allow use of adjoint matrix for reconstruction and iteration, and whether to ask the higher precision between the weight to CG (conjugate gradient) choice. If CG = 0, directly to reconstruction images by IFDST transform. If CG = 1, through the Adjoint matrix (Adjoint FDST) for reconstruction. Finally, we get to de-noised image.

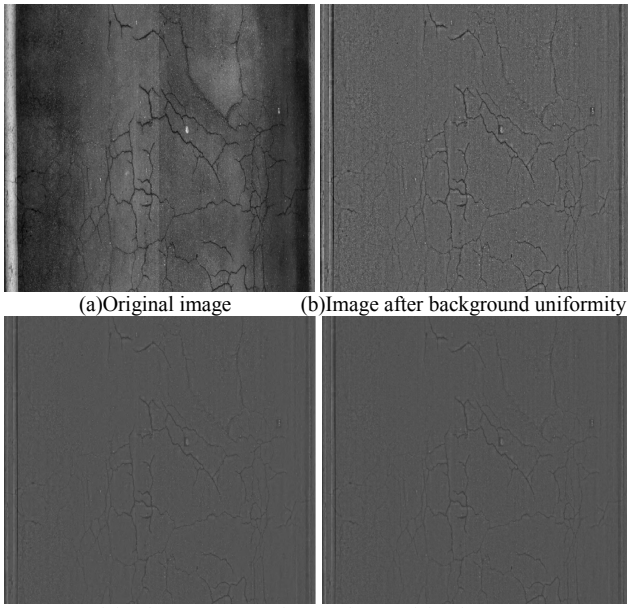

(a)Original image (b)Image after background uniformity

(c) De-noising by Bayes Wavelet (d)De-noising by SURE-FDST

Fig.3 the result by de-noising

We can see from the Fig3 that the SURE-FDST have better sparse expression ability at the edge of the images and the texture's geometric structure characteristics. The FDST frame structure is very simple, and the transform energy more focused, and more faster, to the benefit of further analysis and extract the geometrical characteristics of the image.

IV. CLASSIFICATION BY RADON TRANSFORM

After the procedure is completed, the next phase is to use the obtained image to classify the crack. Radon transform utilizes a set of projections at different angles in an image f(x, y). The resulting projection is the sum of the intensities of the pixels in each direction, i.e. a line integral. The Radon transform can be defined in many different ways, on a more general form the linear Radon transform can be defined as follows:

$$\bar{g}(\xi_0, \xi_1, \xi_2) = \int_{-\infty}^{\infty}\int_{-\infty}^{\infty} g(x,y)\delta(\xi_0 - \xi_1 x - \xi_2 y)\,dxdy \quad (5)$$

Where is the Dirac delta function $\delta(\cdot)$.

To better understand the different types of typical cracks are simulated by considering white lines on a black background, as shown on the below of the figure4:

From Figure4 (a), it can be seen that a peak at 90° in the radon transform indicates a transverse crack on a pavement, and the x coordinate of the peak determines the position of the crack. Similarly, a peak at 0° in Figure4(b) indicates a longitudinal crack, and a peak at 135° in Figure4(c) indicates a diagonal crack at 45°.

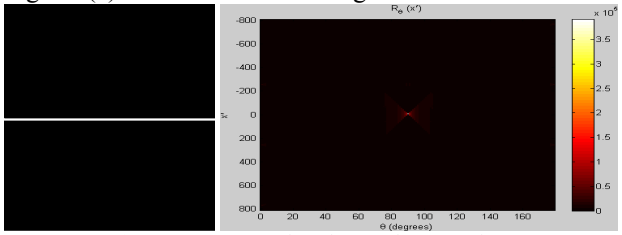

(a) Transverse Crack and Its Radon Transform

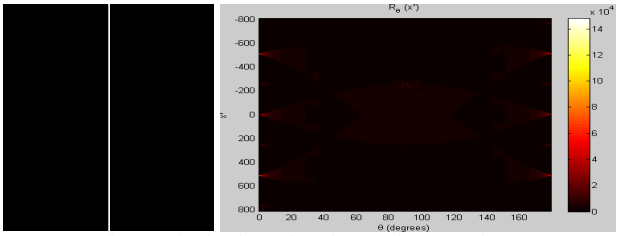

(b) Longitudinal Crack and Its Radon Transform

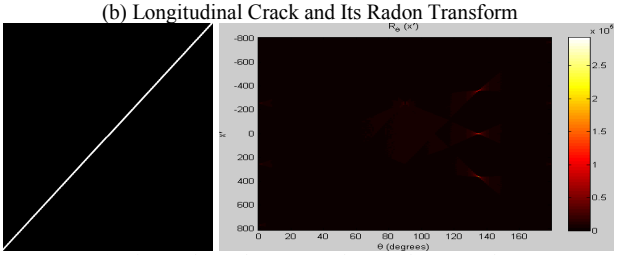

(c) Diagonal Crack at 45° and Its Radon Transform

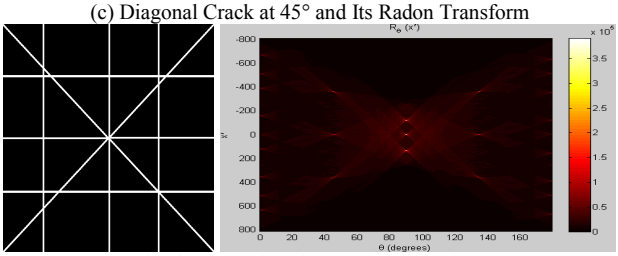

(d) Block Crack and Its Radon Transform

Fig.4 Different types of typical cracks and Its Radon Transform

For the block cracks shown in Figure4(d), there should be one peak array at 0° and another one at 90°. Generally, the number of peaks corresponds to the number of cracks, and the number can be used to determine the type of cracks as a single crack or multiple cracks.

In the Radon transformation, the horizontal ordinate used to classify cracks, vertical coordinates used to locate the cracks, and through the Radon transformation, we can also determine the length and width of crack, so as to the decision the severity of the cracks, and relevant the peak value.

The classification rules as follows:

1) If there is one peak, when 1º< θ <10º or145º< θ <180º, its longitudinal crack; If 80º< θ <100º, its transverse cracks; otherwise its diagonal crack.

2) If there are two or three peaks, classify each of they by the step1.

3) If there are four peaks, two of them located at (1º< θ <10º) and (145º< θ <180º), the other two located at (80º< θ <100º), its block cracks. Else, do step1.

4) If there are five peaks or larger than five, Go to step3 to determine whether is block cracks. If not, its alligator cracks.

5) If the peaks more than ten, it most likely alligator cracks.

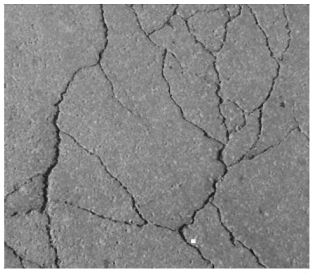

(a) original image

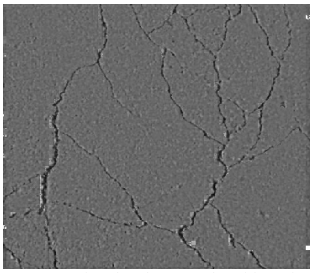

(b) Image after background uniformity

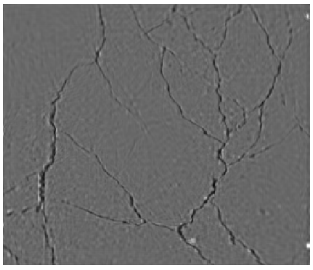

(c)De-noising by SURE-FDST

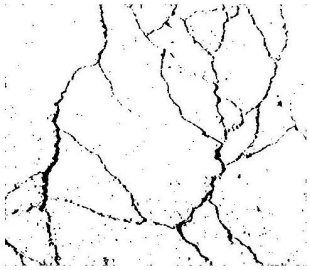

(d)Converting into binary image

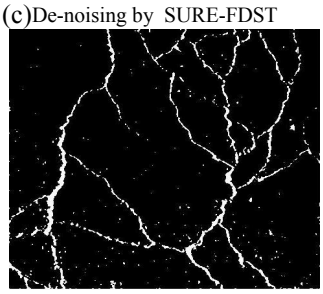

(e)Reversing the intensities

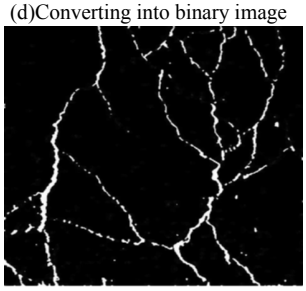

(f) Remove singular points by median filter

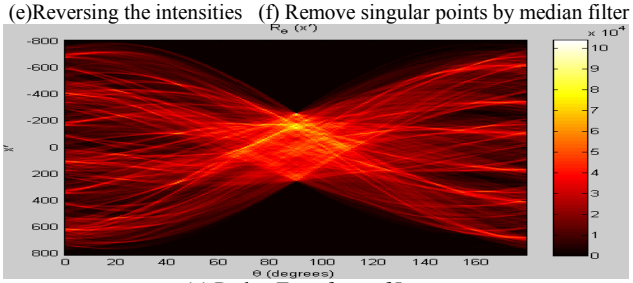

(g) Radon Transform of Image

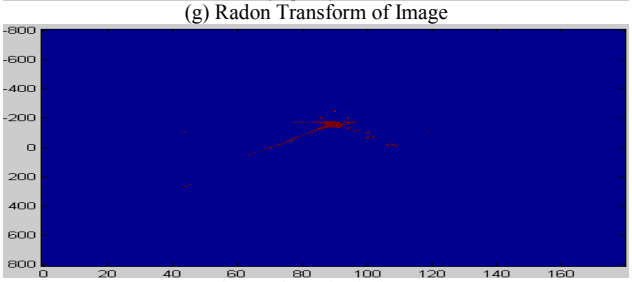

(h)Number of Windows

Fig.5 the result by de-noising

In the Figure5, we use a Composite cracks to test. After background uniformity and SURE-FDST de-noising, and obtain binary image by threshold processing, then reversing the intensities and remove singular points by median filter. Finally, do radon transform to the binary image. We can see from the Figure5(g) and (h), the range of θ is about 65º< θ <110º, so its alligator cracks.The value of peak is 1.0421e+005.

V. SCATTERING TRANSFORM FOR TEXTURE FEATURE MATCHING

A scattering vector is a local descriptor including multi-scale and multi-direction co-occurrence information. It is computed with a cascade of wavelet decompositions and complex modulus[11].Scattering operators recover the lost high frequencies and retransform them into co-occurrence coefficients at multiple scales and orientations. They provide much richer descriptors of complex structures such as corners, junctions and multi-scale texture variations. These coefficients are locally translation invariant and they linearize small deformations.

They are computed with a convolution network[12]which cascades contractive wavelet transforms and modulus operators. Scattering operators provide new representations of stationary image textures, which can discriminate texture having the same power spectrum.

Several authors[13]observed that approximate SIFT feature vectors are computed more efficiently by averaging directly the partial derivative amplitudes of f along the directions of K, with a low-pass filter ϕ_J. These averaged partial derivative amplitudes can be written as averaged wavelet coefficients: $\left|f * \psi_{j,\Upsilon}\right| * \phi(x)$,with a partial derivative wavelet $\psi(x) = \partial g(x) / \partial x_1$,with $g(x) = e^{-|\infty|^2/2}$ and $x = (x_1, x_2)$.

Because Gabor has the better frequency resolution and the direction of resolution for more complex structure texture identification. So we choose complex Gabor for scattering transform. Complex Gabor obtained through frequency modulation of gaussian window :

$$\psi(x) = e^{i\xi x_1} e^{-|x|^2/2} \tag{6}$$

For the fixed texture, because of averaging kernel ϕ_J, the random variability of $\left|f * \psi_{j,\Upsilon}\right| * \phi(x)$ will reduce.

We can achieve local invariability by the way of averaging, reduce the invariability and multi-scale of textons for the descriptor of SIFT, but will reduce information. Scattering operator can restore the lost parts of information in the process of averaging the Co-occurrence coefficient. Scattering coefficient convolution with ϕ_J will produce the second order coefficient of local translation invariability, and can further restore the high frequency information by regularization processing with ϕ_J to the amplitude of fine scales of coefficient. the vector coefficient after q times iteration at the point of x:

$$S_{q,J} f(x) = \left(\left\| f * \psi_{j_1,\Upsilon_1} \right| * \ldots * \left| \psi_{j_q,\Upsilon_q} \right| * \phi_J(x) \right) \tag{7}$$

Where $j_1 < \ldots < j_q < J$, $(\Upsilon_1, \ldots, \Upsilon_q) \in \Gamma^q$. We together all coefficients of the order Meet the conditions of $q \le m$ will get :

$$S_J f(x) = \left(S_{q,J} f(x) \right)_{0 \le q \le m} \tag{8}$$

Scattering transform definition a certain distance between the two images f and g, and have important stability and invariance. Suppose $\left|S_J f(x)\right|^2$ is square of Euclidean norm of the vector $S_J f(x)$, the Scattering distance between the two images f and g is:

$$\left\| S_J f - S_J g \right\|^2 = \int \left| S_J f(x) - S_J g(x) \right|^2 dx \tag{9}$$

The energy of f is transfer in each order of Scattering coefficient, and has a fast decay as the Co-occurrence order 1, 2, and 3. In application, wo shall thus limit the scattering order to m=2.

This paper scattering descriptors used Gabor wavelet which $\xi = 3\pi/4$, the angle of Gabor is $k\pi/K$ ($0 \le k < K = 6$), and low-pass filter is Gaussian filter $\phi_J(x) = \lambda_J \exp\left(-\left(3x/2^{J+1}\right)^2/2\right)$, where $\int \phi_J(x) dx = 1$.

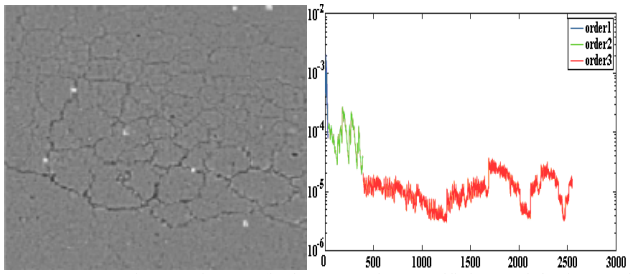

(a)image f (b)the Scattering coefficient of the image f

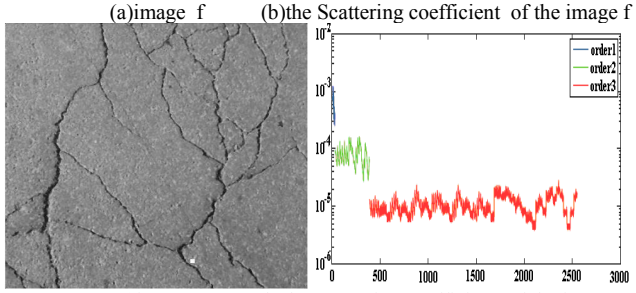

(c)image g (b)the Scattering coefficient of the image g

Fig.6 Scattering coefficient of different texture pavement

Figure 6 shows the scattering coefficient of the natural texture in the m=3. q=1 corresponding the scattering coefficient of blue, and green corresponding q = 2, the scattering coefficient of red corresponding q=3. We can obviously seen in q=2, q=3, they are obviously different scattering coefficient, because of they are different pavement disease types.

Textures having same mean and same power spectrum have nearly the same scattering coefficients of order q = 0 and q = 1. However, different textures typically have co-occurrence coefficients of order $q \ge 2$ which are different. Let $S_{q,J} F_i$ be the vector of scattering coefficients of order q for a texture F_i. The distance of scattering vectors of order q for two textures F_1 and F_2 is normalized by their variance $\sigma^2\left(S_{q,J} F_i\right)$:

$$\rho_q(F_1, F_2) = \frac{\left| E\left\{S_{q,J} F_1\right\} - E\left\{S_{q,J} F_2\right\} \right|^2}{\sigma^2\left(S_{q,J} F_1\right) + \sigma^2\left(S_{q,J} F_2\right)} \tag{10}$$

So, we can through the scattering distance distinguish the textures which have the same power spectrum.Have this method, we can match the same type distresses which is the results of the previous classification, if value of the distance of scattering coefficients between the same distresses is zero, can be determined for the same type of disease. This can greatly improve precision.

In this article, we adopt the images took from complete cross section +S308 line-up-lane1 of WuWei city of GanSu province. The height of CCD line scanning

camera on the pavement inspection vehicle is two meters, and the angle shooting is vertical. The speed of vehicle is 60km/h, and the resolution is 1280*1024. We choose 100 images for the testing, the results are shown below:

TABLE I. PERFORMANCE COMPARISON FOR THE TWO WAYS

The ways	The type of crack				
	transverse	*longitudinal*	*diagonal*	*block*	*alligator*
Detection Without Scattering transform	90.3	89.6	93.5	88.8	92.2
Detection With Scattering transform	92.0	92.0	92.0	92.0	96.0

We can see from the table1, as verification by scattering transform for the results of classification of section IV, the precision of transverse, longitudinal, diagonal, block and alligator are all improved.

VI. CONCLUSIONS

The research presented in this article is aimed at the development of an automated images system for distress detection and classification in pavement images. First to put forward an enhancement algorithm to remove uneven illumination within the pavement images, and then use an shearlet frame to de-noise for the images of uniform. This method can keep image edge features at the same time remove the the singularity of images, and contribute to the next step of binary image. In this paper, Radon transform has been used for line and angle detection about pavement distress of binary images, and the method can be very good at classification of linear distress. Finally the scattering transform was used for verify the result of classification, in order to improve the precision of the classification. This automatic image system with high precision and structure is simple, but only to the linear distress of transverse, longitudinal, diagonal, block and alligator .For more complex diseases such as pothole, etc, which do not have ability to detection, this needs to be improved later

REFERENCES

[1] Roberts,C.A.&Attoh-Okine,N.O.A comparative analysis of two artificial network using pavement performance prediction[J], Computer Aided Civil and In-fras structure Engineering, 1998, 13(5), 39-48

[2] Jitprasithsiri, S, Lee, H.&Sorcic, R.G.Development of digital image processing algorithm to compute a unified crack index for Salt Lake City[J], Transportation Research Record, 2005, No.1526, 142-148

[3] Huang,Y.H, pavement Analysis and Design[M]. Prentice Hall, Englewood Cliffs, NJ, 2005, 15-28

[4] Cheng, H. D., Glazier, C., & Hu, Y. G. (). Novel approach to pavement craking detection based on fuzzy set theory. Journal of Computing in Civil Engineering, 2006, 13(3), 270-280.

[5] Hsu, C. J., Chen, C. F., Lee, C., & Huang, S. M. Airport pavement distress image classification using moment invariant neural network. In 22nd Asian conference on remote sensing and processing (CRISP), Singapore. 2001, 57-64

[6] Zhou, J., Huang, P. S., & Chiang, F.-P. Wavelet-based pavement distress detection and evaluation. Optical Engineering, 2006, 45-56. doi:10.1117/1.2172917.

[7] Sorncharean, S., & Phiphobmongkol, S. Crack detection on asphalt surface image using enhanced grid cell analysis. In 4th IEEE International Symposium on Electronic Design, Test and Applications , 2008, pp. 49 – 54

[8] Wang, K. C. P. Wavelet-based pavement distress image edge detection with Trous algorithm. Transportation Research Record: Journal of the Transportation Research Board , 2008, pp. 73–81

[9] Cheng, H.D., Jiang, X.H.&Glazier,C., Novel approach to pavement cracking detection based on neural network[J], Transportation Research Board, 2001, No.1764, 119-127

[10] Easley G, Labate D, LimWQ. Sparse directional image representation using the discrete shearlet transform[J]. Applied and Computational Harmonic Analysis, 2008, 25(1):25-46

[11] J.Bouvrie, L. Rosasco,T.Poggio: "On Invariance in Hierarchical Models", NIPS 2009, 556-578

[12] Y.LeCun, K. Kavukvuoglu and C. Farabet: "Convolutional Networks and Applications in Vision", Proc.of ISCAS 2010, 78-112

[13] S. Mallat, "Recursive Interferometric Representation", Proc. of EUSICO conference, Denmark, August 2010, 523-544